Journal of Environmental Science International
29(12); 1171~1184; December 2020

pISSN: 1225-4517 eISSN: 2287-3503
https://doi.org/10.5322/JESI.2020.29.12.1171

ORIGINAL ARTICLE

Green Synthesis of Nanoparticles Using Extract of *Ecklonia Cava* and Catalytic Activity for Synthetic Dyes

Beomjin Kim, Woo Chang Song, Sun Young Park[1)], Geuntae Park[*]

Department of Nano Fusion Technology, Pusan National University, Busan 46241, Korea
[1)]Bio-IT Fusion Technology Research Institute, Pusan National University, Busan 46241, Korea

Abstract

The green synthesis of inorganic nanoparticles (NPs) using biomaterials has garnered considerable attention in recent years because of its eco-friendly, non-toxic, simple, and low-cost nature. In this study, we synthesized NPs of noble metals, such as Ag and Au using an aqueous extract of a marine seaweed, *Ecklonia cava*. The formation of AgNPs and AuNPs was confirmed by the presence of surface plasmon resonance peaks in UV-Vis absorption spectra at approximately 430 and 530 nm, respectively. Various properties of the NPs were evaluated using characterization techniques, such as dynamic light scattering, transmission electron microscopy, energy-dispersive X-ray spectroscopy, Fourier transform infrared spectroscopy, and X-ray diffraction analysis. Phytochemicals in the seaweed extract, such as phlorotannins, acted as both reducing and stabilizing agents for the growth of the NPs. The green-synthesized AgNPs and AuNPs were found to exhibit high catalytic activity for the decomposition of organic dyes, including azo dyes, methylene blue, rhodamine B, and methyl orange.

Key words : Green synthesis, Silver nanoparticles, Gold nanoparticles, *Ecklonia cava*, Catalytic activity

1. Introduction

Since the beginning of the 21st century, interest in nanotechnology has continually increased, resulting in the rapid technological development. Nanotechnology is applied in almost every industry, including electronics, medicine, biotechnology, environmental conservation, and energy. Noble metal inorganic nanoparticles (NPs), such as Ag and Au, play important roles in industry because their characteristics vary with their size (Al-Thabaiti et al., 2015; Rathi et al., 2015).

There are physical and chemical methods of synthesizing NPs (Jensen et al., 2000; Lu et al., 2003; Tsuji et al., 2003; Moldovan et al., 2015; Chandrasekaran et al., 2016). However, these methods are expensive and utilize harmful chemicals that contaminate NP surfaces. These NPs are difficult to employ in the environmental and medical fields (Jiménez et al., 2018). NPs produced by eco-friendly synthesis using plant extracts have received considerable attention in recent years as an alternative to in organic NPs. The waste products from the plant extracts serve as reducers and stabilizers, making them easier to use than the products of chemical methods and they do not contain toxic chemicals.

Research into the synthesis of eco-friendly inorganic

Received 10 June, 2020; **Revised** 29 July, 2020;
Accepted 19 August, 2020
[*]**Corresponding author**: Geuntae Park, Department of Nanofusion Technology, Graduate School, Pusan National University, Busan 46241, Korea
Phone : +82-51-510-3740
Email : gtpark@pusan.ac.kr

NPs via various plant extracts is currently underway. Among these natural extracts, brown algae *Ecklonia cava* (EC), which contains phlorotannins (such as phloroglucinol, eckol, and fucodiphloroethol G) as the main active compounds as well as and three sterols (fucosterol, cholesterol, and ergosterol) (Li et al., 2009; Kang et al., 2012a; Kang et al., 2012b; Choi et al., 2015). EC has excellent antibacterial, antioxidant, and anti-cancer properties (Athukorala et al., 2006; Kim et al., 2006; Kong et al., 2009; Choi et al., 2010; Ferreres et al., 2012) and is also produced for consumption. Moreover EC has a higher metal uptake than other microorganisms (Kim et al., 2006; Romera et al., 2007; Mata et al., 2008).

Dyes are widely used in various industries, such as cosmetics, food, and textiles. However, these dyes can be fatal to living organisms as they can lead to carcinogenesis and neurotoxicity in the skin, eyes, and respiratory tract. These dyes are environmental pollutants that are almost non-degradable in nature. Therefore, it is necessary degrade dye contaminants present in the natural environment.

In this study, silver nanoparticles (AgNPs) and gold nanoparticles (AuNPs) were synthesized via an eco-friendly method using EC. Three dyes solutions that are widely used in the dyeing industry, methylene blue (MB), rhodamine B (RB), and methyl orange (MO) were tested for their catalytic activity using sodium borohydride ($NaBH_4$). This experiment was carried out to determine whether the synthesized NPs performed well as catalysts to degrade environmental pollutants.

2. Materials and methods

2.1. Chemicals and reagents

EC was obtained from JEJU TECHNOPARK Inc. (Jeju, Korea). Hydrogen tetrachloroaurate (III) trihydrate ($HAuCl_4 \cdot 3H_2O$), silver nitrate ($AgNO_3$), MB, RB, MO, and NaBH4 were purchased from Sigma -Aldrich Inc. (St. Louis, USA).

2.2. Preparation of EC extract

EC was collected from Jeju Island, Jeju Province, Korea. Botanical identification was performed by Dr. Mook Jae Lee (JEJU TECHNOPARK Inc., Korea), and a sample specimen was deposited at the herbarium of the Jeju Biodiversity Research Institute, Jeju, Korea. The dried EC was homogenized into a fine powder using an electric mixer (HMF-3100S, Hanil Electric, Seoul, Korea). The EC solution was prepared by dissolving the powder in 80% ethanol at room temperature. It was then filtered and concentrated using a rotary vacuum evaporator (Buchi Rotavapor R-144, Buchi Labortechnik, Flawil, Switzerland). The EC extract (50 mL) was powdered via freeze-drying. The powder was then stored at -75°C until further use. For the experiments, this powder was dissolved at a concentration of 4 mg/mL and passed through a syringe filter (0.2 μm) for sterilization.

2.3. Green synthesis of AgNPs and AuNPs

First, 1 mL of the filtered EC extract (2 mg/mL) was added to 1 μL of 1 M $AgNO_3$ solution and incubated in a water bath at 80°C. After 15 min, the suspension was transferred to an icebox filled with ice for 5 min. Similarly, for the synthesis of AuNPs, 1 mL of the filtered EC extract was added to 1 M $HAuCl_4 \cdot 3H_2O$ solution, and the processes used for AgNP synthesis were followed thereafter.

2.4. Characterization of EC–AgNPs and EC–AuNPs

UV-visible spectra were recorded using an Ultrospec 6300 pro (Amersham Biosciences, UK). The particle size of the dispersions and zeta potential were analyzed using a Zetasizer, Nano-ZS90 (Malvern Panalytical, UK). A TALOS F200X system (Thermo Scientific, Waltham, USA) operating at 200 kV was used to obtain high resolution-transmission electron microscopy (HR-TEM) images. The AgNPS and AuNPs were loaded onto a carbon-coated copper grid (Formvar/ Carbon, 200 Mesh, Electron Microscopy Sciences, Hatfield, USA). The dried powders of the lyophilized

AgNPs and AuNPs were retrieved for X-ray diffraction (XRD) analysis and Fourier transform infrared (FT-IR) spectroscopy. XRD measurements were performed using an X'Pert^3 Powder (Malvern Panalytical, UK) X-ray diffractometer. The instrument was operated at 40 kV with a current of 30 mA and Cu Kα radiation (1.540 Å) between 2θ angles of 30° and 80° to analyze the peak data and crystal structure. FT-IR spectroscopy analysis of the AgNPs and AuNPs was carried out using the potassium bromide pellet method. The spectra were recorded using the transmittance mode of a Spectrum GX (Perkin Elmer, Waltham, USA) operating at a resolution of 4 cm^{-1} to determine the phytochemicals present in the EC extract that are responsible for reduction during AgNPs and AuNPs synthesis.

2.5. Catalytic activity of AgNPs and AuNPs

The catalytic activity of the synthesized AgNPs and AuNPs was analyzed based on the UV-Visible spectra of three dyes (MB, RB, and MO) in the presence of ice cold $NaBH_4$. $NaBH_4$ solutions were freshly prepared prior to the experiments. Then, 2 mL aqueous solutions of MB (0.08 mM) and RB (0.05 mM) were mixed with 1 mL $NaBH_4$ (10 mM) and AuNP(or AgNP) solutions. Next, 2 mL of MO aqueous solution was mixed with 1 mL $NaBH_4$ (50 mM) and AuNP(or AgNP) solutions. The volume of the EC-AuNP solution added to each of the mixtures was 15 μL, except for the solution with RB, which contained 10 μL of the EC-AuNP solution. The EC-AgNP solution was added to the mixture at different volumes of (150, 30, and 15 μL) for MB, RB, and MO, respectively. The NP volume was varied in order to observe the process of degradation within minutes.

The reaction kinetics were evaluated by assuming the concentration of reactive dyes to obey the pseudo-first order kinetics, where the integrated form is as follows:

$$-kt = \ln \frac{A_t}{A_0}$$

We calculated the rate constant (k) from the initial absorbance of the dyes (A_0) and the absorbance at time t (A_t).

3. Results and Discussion

3.1. Green synthesis of EC-AgNPs and EC-AuNPs and UV-Vis spectral analysis

The AgNPs and AuNPs formed using the EC extract to reduce metal salts were investigated to evaluate their potential. The addition of the EC extract to the $AgNO_3$ solution resulted in a color change from light yellow to dark brown within 15 min resulting from the formation of colloidal AgNPs. Moreover the UV-vis spectra confirmed the presence of metal NPs because of Surface Plasmon Resonance (SPR). The maximal absorbance peaks of EC and EC-AgNPs appeared at 300 nm and 430 nm, respectively, over the wavelength range of 300 ~ 800 nm. (Fig. 1(a, b)). Similarly, the color of the EC extract changed from light yellow to purple within 15 min after $HAuCl_4 \cdot 3H_2O$ was added. The SPR peak at 530 nm indicated the formation of AuNPs (Fig. 1(c)).

3.2. DLS and HR-TEM analysis

Fig. 2 shows the size distribution of the synthesized AgNPs and AuNPs, with average diameters of 119.7 ± 1.65 and 12.4 ± 1.77 nm, respectively. The zeta potential observed were -22.1 ± 0.36 and -23.2 ± 1.33 mV for EC-AgNPs and EC-AuNPs, respectively.

The morphology, shape, and dispersion of the green -synthesized NPs were observed through HR-TEM. Fig. 3(a-h) shows the TEM images of EC-AgNPs and EC-AuNPs. The majority of the AgNP and AuNPs were slightly spherical in shape NPs with other shapes, such as hexagonals, pentagonals, and triangular ones, were also observed. In addition, a clear lattice pattern was observed, indicating that the synthesized NPs were crystalline in nature. The selected area electron diffraction (SAED) pattern at (111), (200), (220), and (311) planes indicates the presence of a face centered

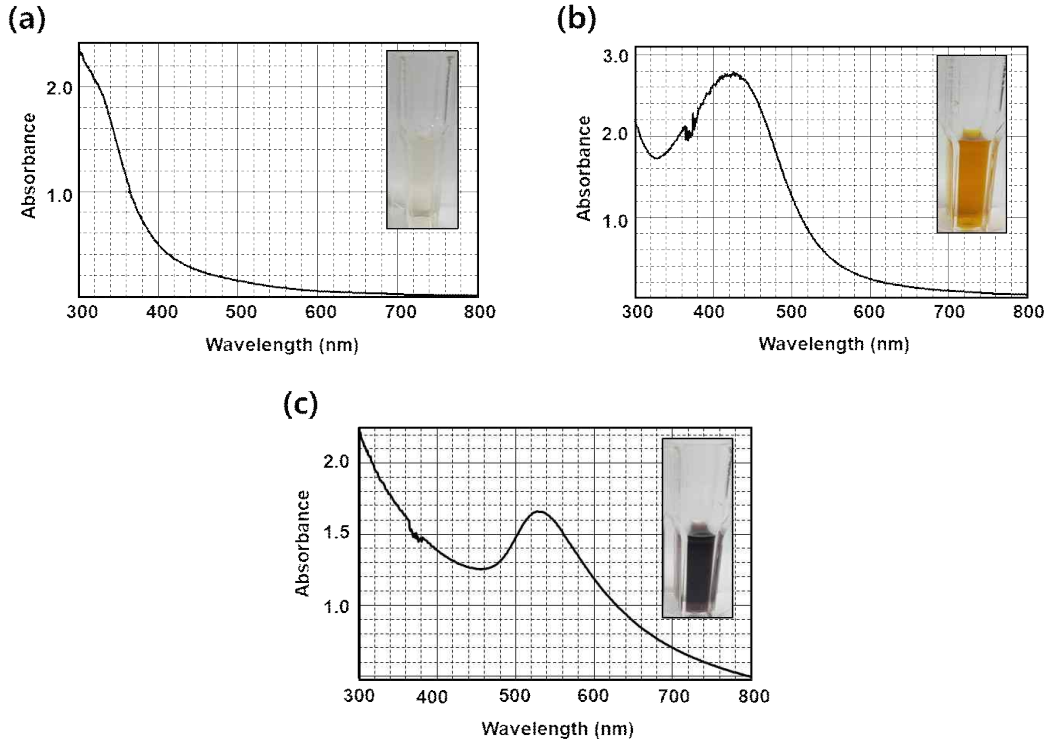

Fig. 1. UV-Vis spectra of EC (a), EC-AgNPs (b), and EC-AuNPs (c).

cubic (FCC) crystal structure (Fig. 3(i, k)).

The energy-dispersive X-ray (EDX) spectra of EC-AgNPs and EC-AuNPs are shown in Fig. 3(j, l). The EDX spectrum of the EC-AgNPs displayed the highest peak at 3 keV, and that of EC-AuNPs exhibited peaks at 2–2.5 and 9.5–10 keV. These results are consistent with those of previous studies (Shahverdi et al., 2007; Arunachalam et al., 2013).

3.3. XRD analysis

Fig. 4 shows the XRD patterns of EC-AgNPs and -AuNPs. In EC-AgNPs, the Bragg reflections at 2θ were observed 38.2°, 44.1°, 64.8°, and 77.3° corresponding to (111), (200), (220), and (311), respectively (Fig. 4(a)). The analysis of EC-AuNPs showed peaks at 2θ values of 38.4°, 44.7°, 64.9°, and 77.9° corresponding to the (111), (200), (220), and (311) planes, respectively (Fig. 4(b)). The lattice planes of crystalline AgNP and AuNPs confirmed that both the bio-synthesized NPs had FCC structures.

3.4. FT-IR spectral analysis

FT-IR spectroscopy was carried out to confirm the role of the EC extract as a reducing and capping agent. The chemical compounds of EC on the surface of the NPs were confirmed by FT-IR spectra. The FT-IR spectra (Fig. 5) showed similar chemical compositions of EC extract (1), EC-AgNPs (2), and EC-AuNPs (3). The FT-IR spectrum of the EC extract shows intense peaks. Other peaks present in the spectrum can be categorized as follows the peak at 3453 cm^{-1} was attributed to the −OH bond extension of alcohols or phenols, while that at 1591 cm^{-1} indicated the N−H bending vibration of amine groups. The peak at 1421

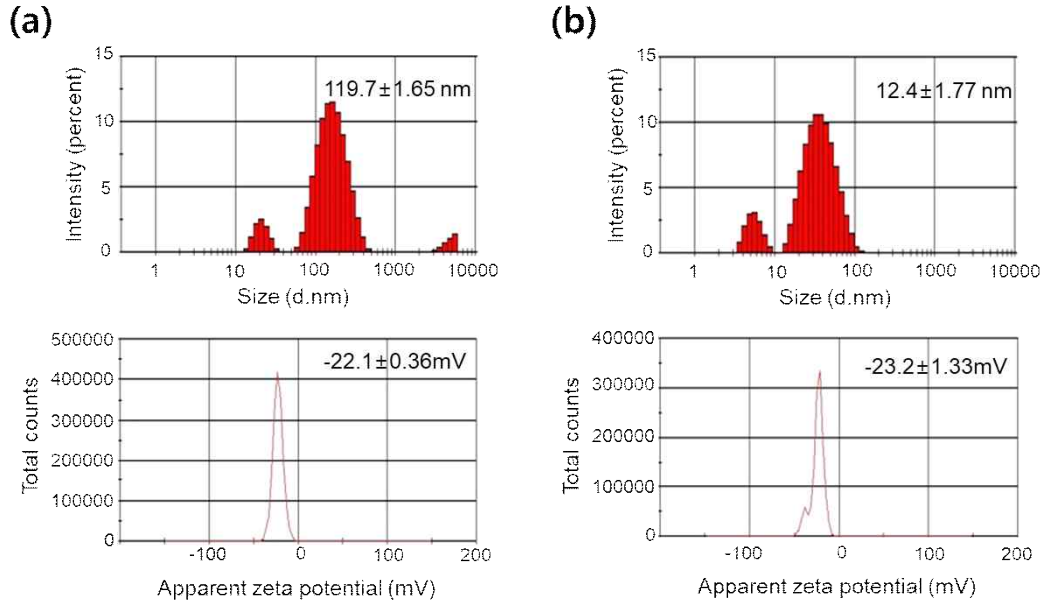

Fig. 2. The size distribution and Zeta potential of synthesized EC-AgNPs (a) and EC-AuNPs (b).

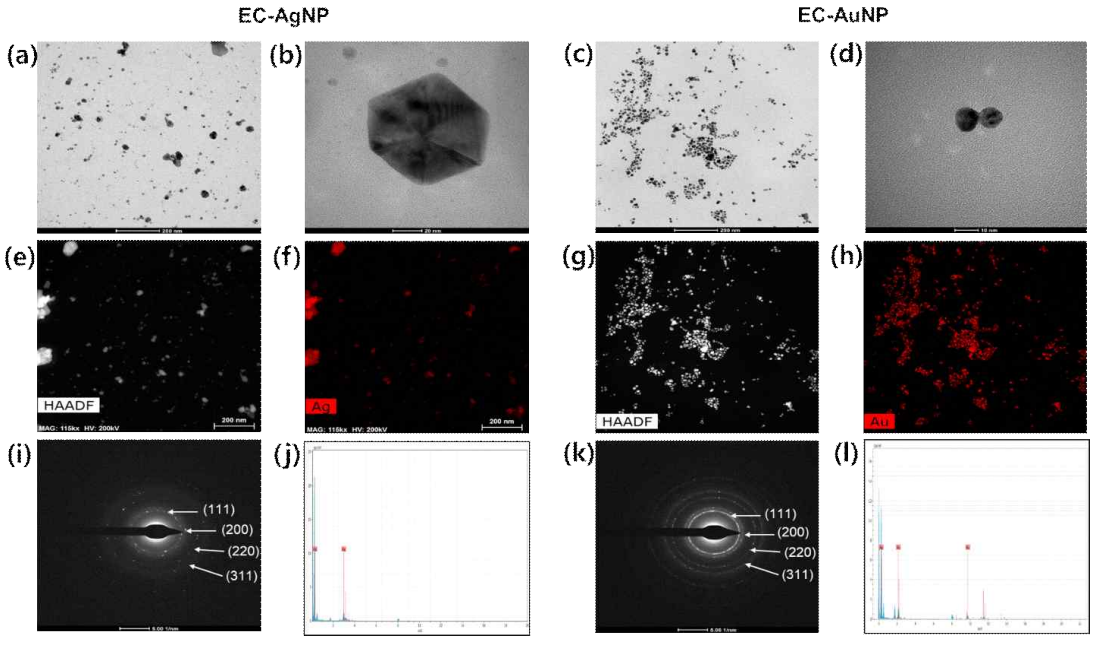

Fig. 3. HR-TEM images of EC-AuNPs (a, b, e, f) and EC-AgNPs (c, d, g, h), SAED patterns of EC-AgNPs (i) and EC-AuNPs (k), and EDX spectra of EC-AgNPs (j) and EC-AuNPs (l).

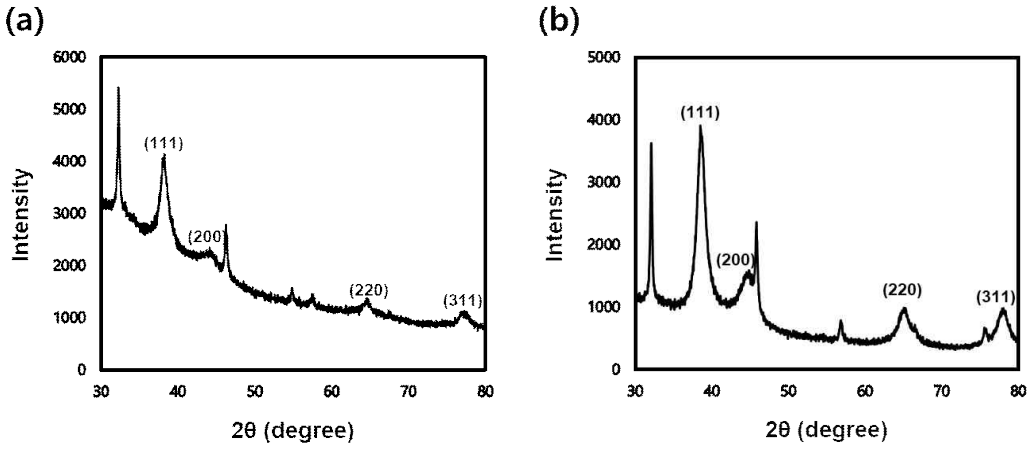

Fig. 4. XRD pattern of EC-AgNPs (a) and EC-AuNPs (b).

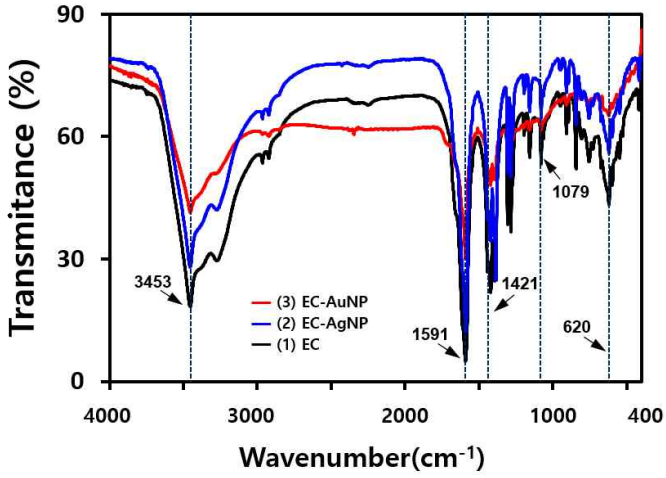

Fig. 5. FT-IR spectra of EC, EC-AgNPs, and EC-AuNPs.

cm^{-1} was attributed to the presence of the −OH bond of polyphenols, a chemical found in algae. The 1079 cm^{-1} peak was attributed to the stretching vibration of C−N in the aromatic ring. After biosynthesis, the NP spectra showed a slight shift in peaks compared to EC. The peak at 1385 cm^{-1} which was only observed in EC-AgNPs corresponds to the N−O stretching vibration of nitro compounds.The peaks of the EC extracts and EC-AuNPs were similar. The difference in the peak at 1385 cm^{-1} suggest that each capping agent of AgNPs and AuNPs could comprise different components. The peaks of EC-AgNPs at 3455, 1590, and 1421 cm^{-1} are assigned to the reduction of the corresponding functional groups. Similarly, the peaks at 3454, 1591, and 1422 cm^{-1} were also observed for EC-AuNPs. This observation suggests that phytochemicals in EC such as polyphenols were responsible for the reduction and stabilization of AgNPs and AuNPs.

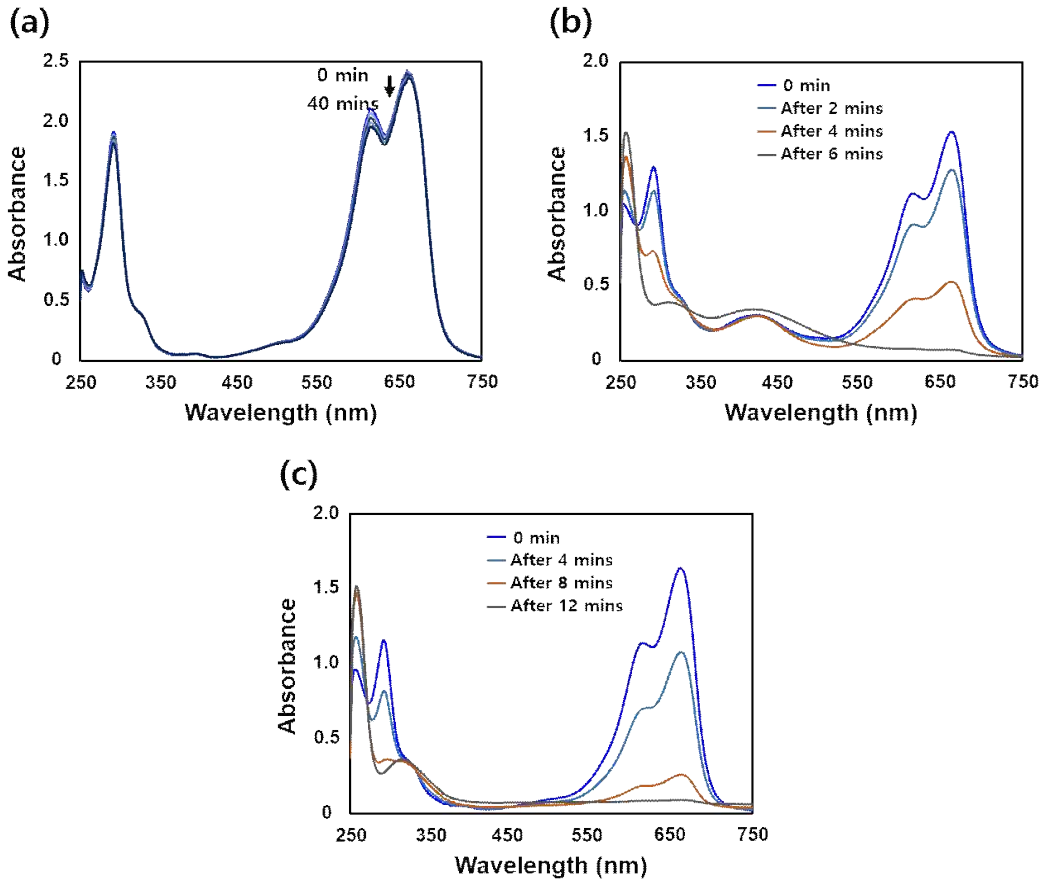

Fig. 6. UV-Vis absorption spectra of MB using different catalysts, only $NaBH_4$ (a), EC-AgNPs (b), and EC-AuNPs (c).

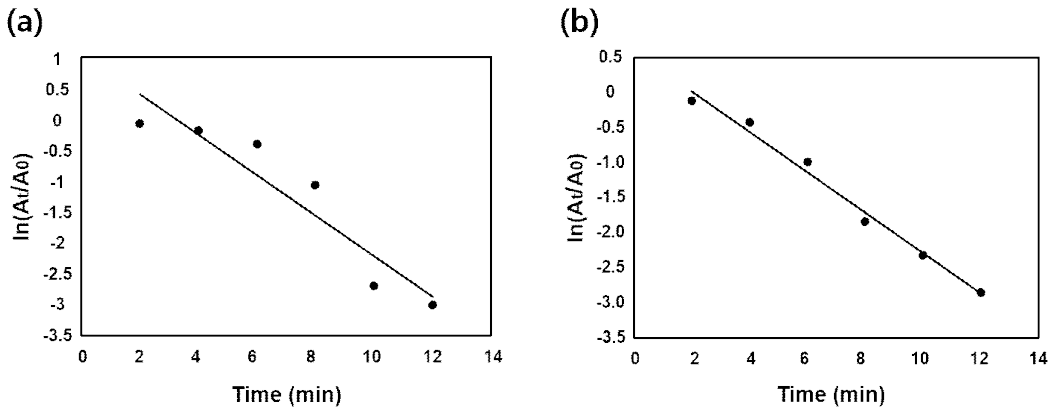

Fig. 7. Graph showing $\ln \frac{A_t}{A_0}$ versus time during MB degradation by EC-AgNPs (a) and EC-AuNPs (b).

Table 1. Values of methylene blue degradation

Dye	Catalyst	Reaction time (min)	Rate constant, k (min^{-1})	Correlation Coefficient, R^2
MB	EC-AgNP	12	0.3264	0.8844
	EC-AuNP	12	0.2883	0.9868

3.5. Catalytic reduction of EC-AgNPs and -AuNPs

MB is a thiazine dye that is mainly used as a remedy for methemoglobinemia and in various other fields (British Medical Association, 2015). It is used as a redox indicator and exhibits good antimalarial activity. RB is a fluorescent dye and is frequently used as a water tracer to determine the rate and direction of transport and flow (Vijayan et al., 2019). MO is an azo dye that has the R−N=N−R′ functional group and is a pH indicator that is commonly used in titration because of its clear and distinct color variance at different pH values. These dyes are generally used in textile, food, and chemical industries. Environmental pollutants discharge in wastewater from these industries are highly toxic, mutagenic, or carcinogenic to the environment, aquatic organisms, and human beings (Asfaram et al., 2017). Therefore, the removal of dyes discharged as water-borne environmental pollutants is desirable. The degradation reactions of these three dyes were investigated and expressed in the following order: MB, RB, and MO. All reactions were monitored using a UV-Vis spectrophotometer.

3.5.1. Reduction of MB

MB is dark blue in color and exhibits a maximum absorbance peak at 662 nm in the UV-Vis spectra. Fig. 6 shows the UV-Vis spectrum of MB reduced in the presence of $NaBH_4$. Although $NaBH_4$ is a strong reducing agent, the characteristic peak of MB remained. $NaBH_4$ could not reduce MB because of the large reduction potential difference between the two solutions. However, when the synthesized EC-AgNPs and EC-AuNPs were added as catalysts, the mixture was gradually reduced and became colorless. UV-Vis spectra of MB indicate that degradation occurred at 2 min intervals using $NaBH_4$ when with EC-AgNPs (150 μL) or EC-AuNPs (15 μL) were used as catalysts (Fig. 6). After addition of EC-AgNPs or EC-AuNPs, the maximum absorbance peak at 662 nm lowered in intensity as the dyes was completely reduced to a colorless leuco form of MB within 12 min. A new peak at approximately 250 nm was observed and was assinged to the formation of the leuco form of MB its intensity increased as the reaction progressed (Vijayan et al., 2019).

This reaction occurred because the reduction potential of the nanocatalysts was between that of MB and $NaBH_4$. Due to the large surface-to-volume ratio of the metal NPs, the reaction was able to commence. In this reaction, $NaBH_4$ was the electron donor and MB was the acceptor. MB was easily reduced by electrons from borohydride on the catalytic surface.

The kinetics of the reaction were studied spectrophotometrically. The rate constant was obtained on the basis of the absorbance at 662 nm over a period of time. We assumed the pseudo-first order kinetics in this study. Fig. 7 displays a graph of $\ln\frac{A_t}{A_0}$ versus time (t). The rate constant (k) was obtained from the slope of the plot. Detailed values are provided in Table 1.

3.5.2. Catalytic reduction of RB

RB solution is pink and exhibits a maximum absorbance at 553 nm. Fig. 8 shows the UV-Vis spectra of RB mixed with $NaBH_4$ in the absence of the catalysts. In the absence of the a catalyst, the maximum absorbance remained almost unchanged.

In addition, Fig. 8 shows the spectra of the solutions

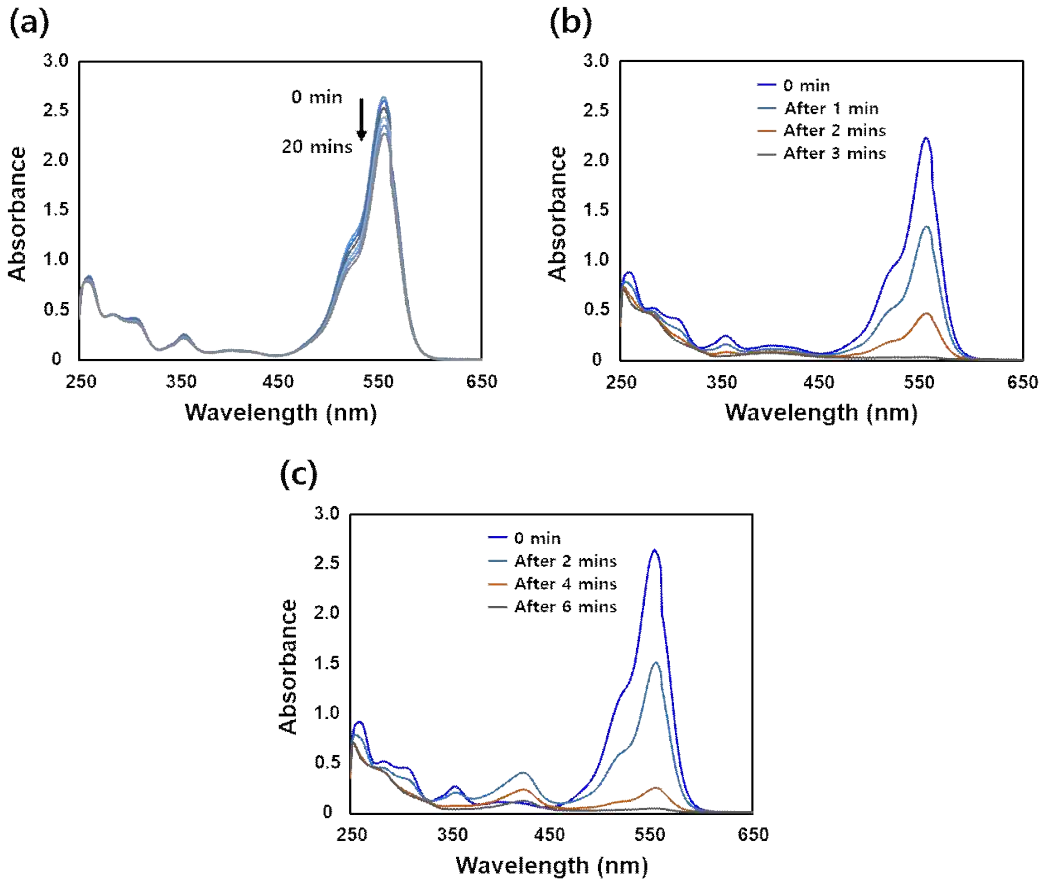

Fig. 8. UV-Vis absorption spectra of RB using different catalysts, only $NaBH_4$ (a), EC-AgNPs (b), and EC-AuNPs (c).

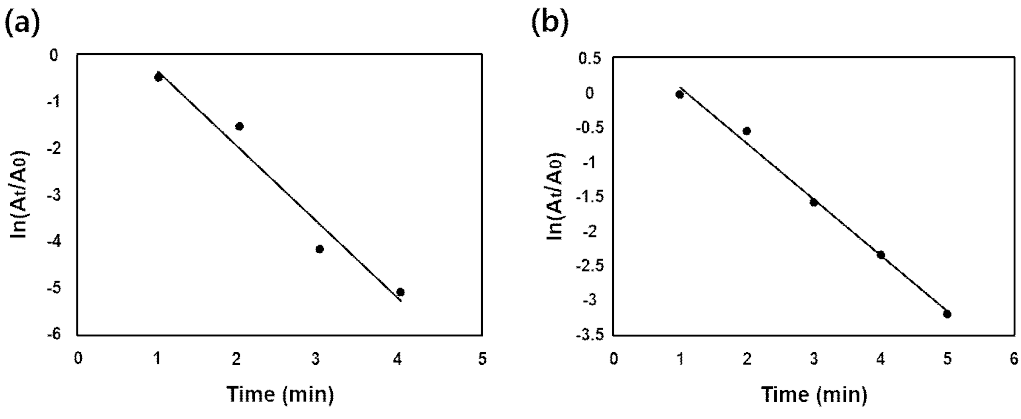

Fig. 9. Graph showing $\ln\frac{A_t}{A_0}$ versus time during RB degradation by EC-AgNPs (a) and EC-AuNPs (b).

Table 2. Values of rhodamine B degradation

Dye	Catalyst	Reaction time (min)	Rate constant, k (min^{-1})	Correlation Coefficient, R^2
RB	EC-AgNP	4	1.6303	0.9615
	EC-AuNP	5	0.8045	0.9929

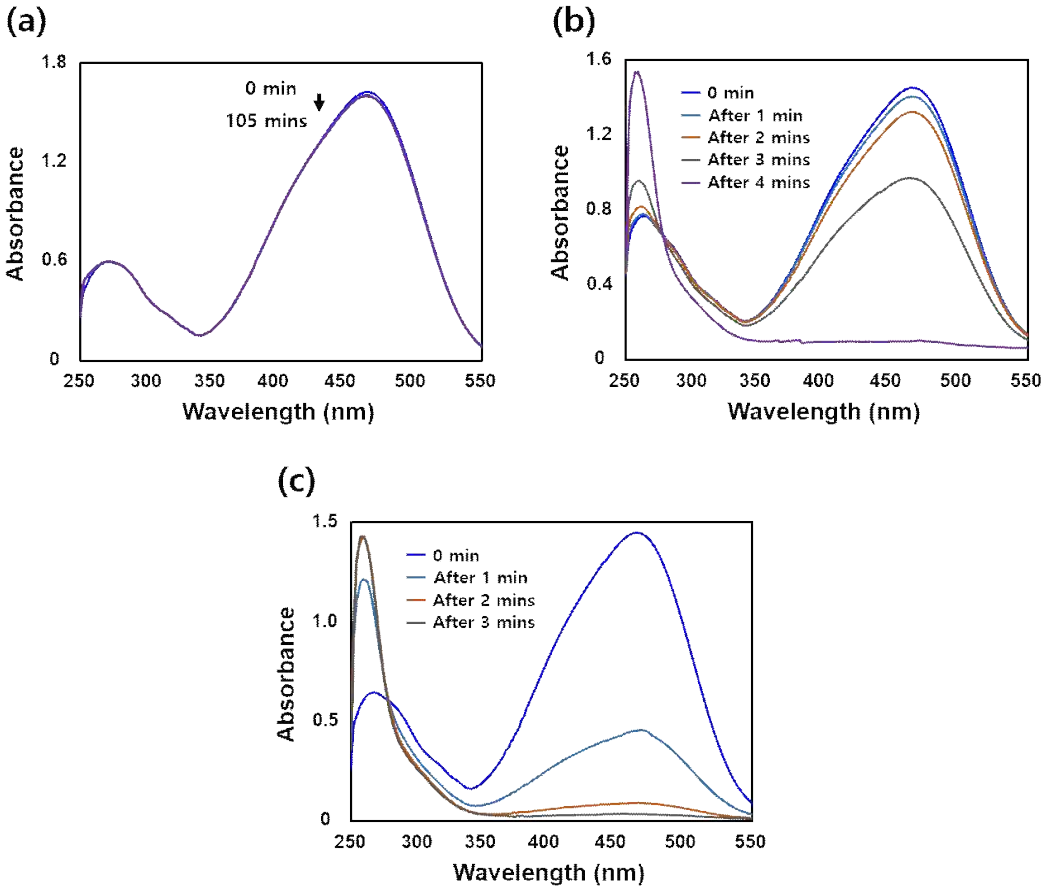

Fig. 10. UV-Vis absorption spectra of MO using different catalysts only $NaBH_4$ (a), EC-AgNPs (b), and EC-AuNPs (c).

undergoing reduction catalyzed by the synthesized EC-AgNPs (30 μL) and EC-AuNPs (10 μL). Measurements at 1 min intervals indicated that the maximum absorbance decreased completely as the mixture became colorless after 4 and 5 min, respectively.

The rate constant (k) was calculated from the absorbance at 553 nm over a period of time. The pseudo-first order kinetics were assumed. A plot of $\ln\frac{A_t}{A_0}$ versus time is shown in Fig. 9. Detailed values of the rate constant (k) are provided in Table 2.

3.5.3. Catalytic reduction of MO

MO is an azo dye that is orange in color. A maximum absorbance peak at 464 nm was observed in the UV-Vis spectrum of MO that underwent the reduction reaction

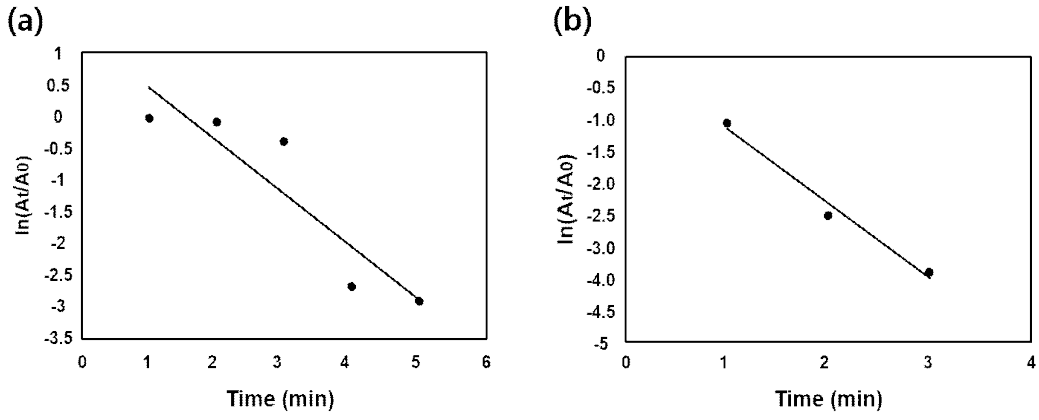

Fig. 11. Graph showing $\ln \frac{A_t}{A_0}$ versus time during MO degradation by EC-AgNPs (a) and EC-AuNP (b).

Table 3. Values of methyl orange degradation

Dye	Catalyst	Reaction time (min)	Rate constant, k (min^{-1})	Correlation Coefficient, R^2
MO	EC-AgNP	5	0.8344	0.8352
	EC-AuNP	3	1.3108	0.9820

using $NaBH_4$ in the absence of catalysts (Fig. 10). The maximum absorbance did not change significantly. The spectra of MO solutions reduced over the synthesized EC-AgNP (5 μL) and EC-AuNP (15 μL) are shown in Fig. 10(b) and 10(c). The maximum absorbance measured at 1 min intervals was found to decrease gradually and the EC-AgNP- and EC-AuNP-containing solutions became colorless within 5 and 3 min, respectively.

The rate constant (k) was calculated from the slope of the plot in Fig. 11, which was generated on the basis of the absorbance values at 464 nm. The pseudo-first order kinetics were assumed in this study. Details are provided in Table 3.

All dyes were reduced to colorless products by $NaBH_4$ with EC-AgNPs or EC-AuNPs as a catalyst within a short time of 12 min. During the degradation of dyes, adsorption occurs between NPs and dye molecules. The green-synthesized metal NPs helped the electrons of $NaBH_4$ move to the dye molecules. Saha et al.(2017) demonstrated that AgNPs acted as a mediators in transferring electrons during MB degradation. Rahman et al.(2013) reported that an electron-hole pair between the valence and conduction bands of NPs caused the RB degradation. In the case of MO, the strong orange color is attributed to the azo group (−N=N−) acting as a chromophorer (Nandhini et al., 2019). The chromophore groups were reduced to colorless amines (−NH−NH−) in the presence of NaBH4 that serves as the reducing agent and the biosynthesized NPs that serve as the catalyst during MO decomposition. The degradation products of MB were leucomethylene blue and RB was reduced to small aliphatic chains, small chain alcohols, and ketones. (AlHamedi et al., 2009, Baldev et al., 2013) MO was cleaved into *N*, *N*-dimethyl-benzene-1, 4-diamine, and 4-aminobenzenesulfonate.

Many previous studies have investigated the catalytic potential of various metal NPs. For instance, Karnan et al.(2016) reported the reduction of MO using ZnONPs

developed from the rambutan (*Nephelium lappaceum*) peel extract. The decomposition of 4-nitrophenol, MB, and MO was demonstrated by Lim and Park(2018) using $NaBH_4$ and in the presence of AuNPs formed using rosmarinic acid. Moreover, Yu et al.(2019) successfully decolorized reactive dyes with $NaBH_4$ and biogenic AgNPs using *Eriobotrya japonica* at various temperatures. In their study, both reactive red 120 and reactive black 5 were decomposed within 30 min.

4. Conclusion

In this study, AgNPs and AuNPs were synthesized at 80°C via a simple and eco-friendly synthetic method using EC extracts. The synthesized EC-AgNPs and EC-AuNPs were characterized by UV-Vis, DLS, HR-TEM, EDX, XRD and FT-IR analyses. UV-Vis and EDX spectroscopies confirmed the formation of AgNps and AuNPs. The size and morphology of the EC-AgNPs and EC-AuNPs were determined using DLS and HR-TEM. The Bragg's reflections from the (111), (200), (220), and (311) planes in the XRD and SAED patterns confirmed that the EC-AgNPs and EC-AuNPs had the FCC structure. FT-IR spectra suggested that EC extracts have an important role as reducing and capping agents in the synthesis and stabilization of NPs. The green-synthesized NPs were employed as effective nanocatalysts for the reduction of MB, RB, and MO in the presence of $NaBH_4$. The reaction was found to be of the pseudo-first order. The rate constant of the decomposition of the dyes was determined by studying the reduction kinetics. In conclusion, algae-based NPs exhibit excellent catalytic activity and reactivity and can serve as inexpensive and environmentally safe catalysts for the degradation of various dye pollutants. Therefore, such NPs can be applied for water purification and in textile industries, especially for environmental remediation.

Acknowledgment

This work was supported by Pusan National University Research Grant, 2019.

REFERENCES

AlHamedi, F. H., Rauf, M. A., Ashraf, S. S., 2009, Degradation studies of rhodamine B in the presence of UV/H_2O_2, Desalination, 239, 159-166.

AL-Thabaiti, S. A., Khan, Z., Hussain, S., 2015, Biogenic silver nanosols: Flavonol based green synthesis, and effects of stabilizers on their morphology, J. Mol. Liq., 212, 316-324.

Arunachalam, K. D., Annamalai, S. K., Hari, S., 2013, One-step green synthesis and characterization of leaf extract-mediated biocompatible silver and gold nanoparticles from *Memecylon umbellatum*, Int. J. Nanomed., 8, 1307-1315.

Asfaram, A., Ghaedi, M., Azqhandi, M. H. A., Goudarzi, A., Hajati, S., 2017, Ultrasound-assisted binary adsorption of dyes onto Mn@ CuS/ZnS-NC-AC as a novel adsorbent: Application of chemometrics for optimization and modeling, J. Ind. Eng. Chem., 54, 377-388.

Athukorala, Y., Kim, K. N., Jeon, Y. J., 2006, Antiproliferative and antioxidant properties of an enzymatic hydrolysate from brown algae, *Ecklonia cava*, Food Chem. Toxicol., 44, 1065-1074.

Baldev, E., MubarakAli, D., Ilavarasi, A., Pandiaraj, D., Ishack, K. A. S. S., Thajuddin, N., 2013, Degradation of synthetic dye, rhodamine B to environmentally non-toxic products using microalgae, Colloids Surf., B, 105, 207-214.

British Medical Association, 2015, British national formulary : BNF 69, 69th ed., Pharmaceutical Press, 34.

Chandrasekaran, R., Gnanasekar, S., Seetharaman, P., Keppanan, R., Arockiaswamy, W., Sivaperumal, S., 2016, Formulation of *Carica papaya* latex-functionalized silver nanoparticles for its improved antibacterial and anticancer applications, J. Mol. Liq., 219, 232-238.

Choi, B. W., Lee, H. S., Shin, H. C., Lee, B. H., 2015, Multifunctional activity of polyphenolic compounds associated with a potential for alzheimer's disease therapy from *Ecklonia cava*, Phytother. Res., 29,

549-553.

Choi, J. G., Kang, O. H., Brice, O. O., Lee, Y. S., Chae, H. S., Oh, Y. C., Sohn, D. H., Park, H., Choi, H. G., Kim, S. G., Shin, D. W., Kwon, D. Y., 2010, Antibacterial activity of *Ecklonia cava* against methicillin-resistant staphylococcus aureus and salmonella spp, Foodborne Pathog. Dis., 7, 435-441.

Ferreres, F., Lopes, G., Gil-Izquierdo, A., Andrade, P. B., Sousa, C., Mouga, T., Valentão, P., 2012, Phlorotannin extracts from fucales charac.terized by HPLC-DAD -ESI-MSn: Approaches to hyaluronidase inhibitory capacity and antioxidant properties, Mar. Drugs, 10, 2766-2781.

Jensen, T. R., Malinsky, M. D., Haynes, C. L., Duyne, R. P. V., 2000, Nanosphere lithography: Tunable localized surface plasmon resonance spectra of silver nanoparticles, J. Phys. Chem. B, 104, 10549-10556.

Jiménez, Z., Kim, Y. J., Mathiyalagan, R., Seo, K. H., Mohanan, P., Ahn, J. C., Kim, Y. J., Yang, D. C., 2018, Assessment of radical scavenging, whitening and moisture retention activities of *Panax ginseng* berry mediated gold nanoparticles as safe and efficient novel cosmetic material, Artif. Cells, Nanomed., Biotechnol., 46, 333-340.

Kang, J. I., Kim, S. C., Kim, M. K., Boo, H. J., Jeon, Y. J., Koh, Y. S., Yoo, E. S., Kang, S. M., Kang, H. K., 2012, Effect of dieckol, a component of *Ecklonia cava*, on the promotion of hair growth, Int. J. Mol. Sci., 13, 6407-6423.

Kang, S. M., Heo, S. J., Kim, K. N., Lee, S. H., Jeon, Y. J., 2012, Isolation and identification of new compound, 2, 7″-phloroglucinol-6,6′-bieckol from brown algae, *Ecklonia cava* and its antioxidant effect, J. Funct. Foods, 4, 158-166.

Karnan, T., Selvakumar, S. A. S., 2016, Biosynthesis of ZnO nanoparticles using rambutan (*nephelium lappaceum* L.) peel extract and their photocatalytic activity on methyl orange dye, J. Mol. Struct., 1125, 358-365.

Kim, M. M., Ta, Q. V., Mendis, E., Rajapakse, N., Jung, W. K., Byun, H. G., Jeon, Y. J., Kim, S. K., 2006, Phlorotannins in *Ecklonia cava* extract inhibit matrix metalloproteinase activity, Life Sci., 79, 1436-1443.

Kong, C. S., Kim, J. A., Yoon, N. Y., Kim, S. K., 2009, Induction of apoptosis by phloroglucinol derivative from *Ecklonia cava* in MCF-7 human breast cancer cells, Food Chem. Toxicol., 47, 1653-1658.

Li, Y., Qian, Z. J., Ryu, B. M., Lee, S. H., Kim, M. M., Kim, S. K., 2009, Chemical components and its antioxidant properties in vitro: An edible marine brown alga, *Ecklonia cava*, Bioorg. Med. Chem., 17, 1963-1973.

Lim, S. H., Park, Y. M., 2018, Green synthesis, characterization and catalytic activity of gold nanoparticles prepared using rosmarinic acid, J. Nanosci. Nanotechnol., 18, 659-667.

Lu, H. W., Liu, S. H., Wang, X. L., Qian, X. F., Yin, J., Zhu, Z. K., 2003, Silver nanocrystals by hyperbranched polyurethane-assisted photochemical reduction of Ag^{+}, Mater. Chem. Phys., 81, 104-107.

Mata, Y. N., Blázquez, M. L., Ballester, A., González, F., Muñoz, J. A., 2008, Characterization of the biosorption of cadmium, lead and copper with the brown alga *Fucus vesiculosus*, J. Hazard. Mater., 158, 316-323.

Moldovan, B., David, L., Achim, M., Clichici, S., Filip, G. A., 2016, A green approach to phytomediated synthesis of silver nanoparticles using *Sambucus nigra* L. fruits extract and their antioxidant activity, J. Mol. Liq., 221, 271-278.

Nandhini, N. T., Rajeshkumar, S., Mythili, S., 2019, The possible mechanism of eco-friendly synthesized nanoparticles on hazardous dyes degradation, Biocatal. Agric. Biotechnol., 19, 101138.

Rahman, Q. I., Ahmad, M., Misra, S. K., Lohani, M., 2013, Effective photocatalytic degradation of rhodamine B dye by ZnO nanoparticles, Mater. Lett., 91, 170-174.

Romera, E., González, F., Ballester, A., Blázquez, M. L., Muñoz, J. A., 2007, Comparative study of biosorption of heavy metals using different types of algae, Bioresour. Technol., 98, 3344-3353.

Saha, J., Begum, A., Mukherjee, A., Kumar, S., 2017, A novel green synthesis of silver nanoparticles and their catalytic action in reduction of methylene blue dye, Sustainable Environ. Res., 27, 245-250.

Shahverdi, A. R., Fakhimi, A., Shahverdi, H. R., Minaian, S., 2007, Synthesis and effect of silver nanoparticles on the antibacterial activity of different antibiotics against *Staphylococcus aureus* and *Escherichia coli*, Nanomedicine, 3, 168-171.

Sre, P. R. R., Reka, M., Poovazhagi, R., Kumar, M. A., Murugesan, K., 2015, Antibacterial and cytotoxic effect

of biologically synthesized silver nanoparticles using aqueous root extract of *Erythrina indica lam*, Spectrochim. Acta, Part A, 135, 1137-1144.

Tsuji, T., Kakita, T., Tsuji, M., 2003, Preparation of nano-size particles of silver with femtosecond laser ablation in water, Appl. Surf. Sci., 206, 314-320.

Vijayan, R., Joseph, S., Mathew, B., 2019, Anticancer, antimicrobial, antioxidant, and catalytic activities of green-synthesized silver and gold nanoparticles using *Bauhinia purpurea* leaf extract, Bioprocess Biosyst Eng, 42, 305-319.

Yu, C., Tang, J., Liu, X., Ren, X., Zhen, M., Wang, L., 2019, Green biosynthesis of silver nanoparticles using *Eriobotrya japonica* (Thunb.) leaf extract for reductive catalysis, Materials, 12, 189

• Graduate student. Beom-Jin Kim
Department of Nano Fusion Technology, Pusan National University
201210503@pusan.ac.kr
• Graduate student. Woo-Chang Song
Department of Nano Fusion Technology, Pusan National University
dck3202@naver.com
• Researcher. Sun-Young Park
Bio-IT Fusion Technology Research Institute, Pusan National University
sundeng99@pusan.ac.kr
• Professor. Geun-Tae Park
Department of Nano Fusion Technology, Pusan National University
gtpark@pusan.ac.kr